Metabolic Engineering Communications 3 (2016) 111–119

Contents lists available at ScienceDirect

Metabolic Engineering Communications

journal homepage: www.elsevier.com/locate/mec

Enhancing muconic acid production from glucose and lignin-derived aromatic compounds via increased protocatechuate decarboxylase activity

Christopher W. Johnson, Davinia Salvachúa, Payal Khanna, Holly Smith, Darren J. Peterson, Gregg T. Beckham *

National Bioenergy Center, National Renewable Energy Laboratory, Golden, CO 80401, United States

ARTICLE INFO

Article history:
Received 1 March 2016
Received in revised form
1 April 2016
Accepted 21 April 2016
Available online 22 April 2016

Keywords:
Protocatechuate decarboxylase
Pseudomonas Putida KT2440
cis,cis-Muconate
Muconic acid
Lignin valorization

ABSTRACT

The conversion of biomass-derived sugars and aromatic molecules to *cis,cis*-muconic acid (referred to hereafter as muconic acid or muconate) has been of recent interest owing to its facile conversion to adipic acid, an important commodity chemical. Metabolic routes to produce muconate from both sugars and many lignin-derived aromatic compounds require the use of a decarboxylase to convert protocatechuate (PCA, 3,4-dihydroxybenzoate) to catechol (1,2-dihydroxybenzene), two central aromatic intermediates in this pathway. Several studies have identified the PCA decarboxylase as a metabolic bottleneck, causing an accumulation of PCA that subsequently reduces muconate production. A recent study showed that activity of the PCA decarboxylase is enhanced by co-expression of two genetically associated proteins, one of which likely produces a flavin-derived cofactor utilized by the decarboxylase. Using entirely genome-integrated gene expression, we have engineered *Pseudomonas putida* KT2440-derived strains to produce muconate from either aromatic molecules or sugars and demonstrate in both cases that co-expression of these decarboxylase associated proteins reduces PCA accumulation and enhances muconate production relative to strains expressing the PCA decarboxylase alone. In bioreactor experiments, co-expression increased the specific productivity (mg/g cells/h) of muconate from the aromatic lignin monomer *p*-coumarate by 50% and resulted in a titer of >15 g/L. In strains engineered to produce muconate from glucose, co-expression more than tripled the titer, yield, productivity, and specific productivity, with the best strain producing 4.92 ± 0.48 g/L muconate. This study demonstrates that overcoming the PCA decarboxylase bottleneck can increase muconate yields from biomass-derived sugars and aromatic molecules in industrially relevant strains and cultivation conditions.

1. Introduction

Muconic acid is an intermediate in the β-ketoadipate pathway employed by many microbes for catabolism of aromatic compounds (Harwood and Parales, 1996; Ornston and Stanier, 1966). There is substantial interest in producing muconic acid from biomass, typically motivated by the ability to efficiently convert muconic acid to adipic acid by catalytic hydrogenation under mild conditions (Vardon et al., 2015). Adipic acid is an industrially important dicarboxylic acid that is a precursor to nylon 6,6, among other polymers. It is conventionally produced by nitric acid oxidation of cyclohexanol and cyclohexanone, releasing nitrous acid. With a market volume of 2.6 million tons per year, adipic acid production contributes substantially to the nitrous acid-mediated generation of ozone-producing free radicals, thus prompting substantial efforts to produce it from renewable resources (Deng et al., 2016; Polen et al., 2013; Van de Vyver and Román-Leshkov, 2013). Recently, it has been shown that *trans,trans*-muconic acid can be converted catalytically to diethyl terephthalate, another important commodity polymer precursor (Lu et al., 2015).

Muconic acid can be produced biologically by dioxygenase enzymes that catalyze intradiol ring-cleavage of catechol, a central intermediate in one branch of the β-ketoadipate pathway (Fig. 1) (Xie et al., 2014). However, many aromatic molecules derived from the depolymerization of lignin, which accounts for 15–30% of the dry weight of biomass, are metabolized through a parallel branch of the β-ketoadipate pathway in which protocatechuate (PCA), rather than catechol, serves as the central intermediate. Employing a PCA decarboxylase, which converts PCA to catechol, has enabled the production of muconate from lignin monomers such as *p*-

* Corresponding author.
E-mail address: gregg.beckham@nrel.gov (G.T. Beckham).

http://dx.doi.org/10.1016/j.meteno.2016.04.002

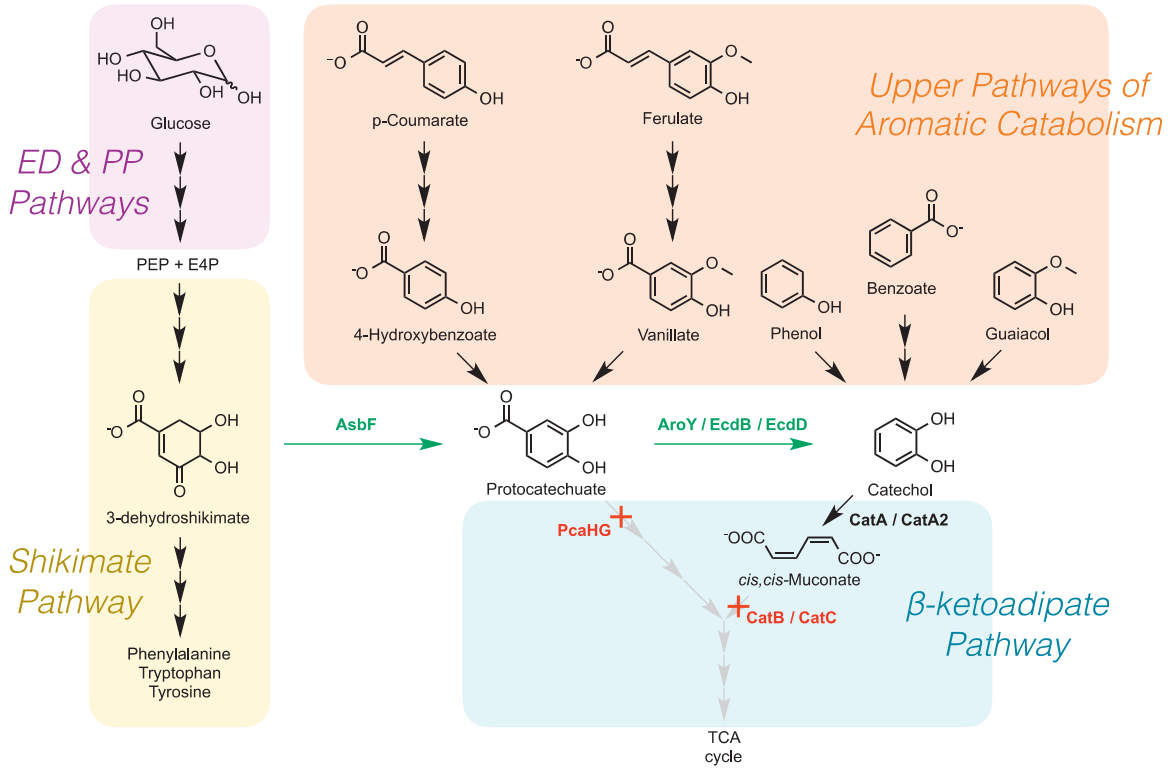

Fig. 1. Metabolic pathways for production of muconate from glucose and lignin-derived aromatic compounds. In *P. putida* KT2440, glucose is metabolized through the Entner-Doudoroff (ED) and pentose phosphate (PP) pathways to produce phosphoenolpyruvate (PEP) and erythrose 4-phosphate (E4P), which can be condensed to enter the shikimate pathway for aromatic amino acid biosynthesis. An intermediate in the shikimate pathway, 3-dehydroshikimate, can be converted to PCA by the action of a 3-DHS dehydratase, such as AsbF from *Bacillus cereus* used here. Deletion of the genes encoding the PCA dioxygenase, PcaHG, and integration of genes encoding the PCA decarboxylase AroY from *Enterobacter cloacae* and two associated proteins, EcdB and EcdD, from enables PCA to be converted to catechol rather than entering the β-ketoadipate pathway. Two paralogous dioxygenases, CatA and CatA2, convert catechol to muconate, which accumulates due to deletion of the genes encoding CatB and CatC, two enzymes required for further metabolism of muconate. Lignin-derived aromatic molecules are metabolized through upper pathways to form catechol in the case of phenol or guaiacol while *p*-coumarate, ferulate, 4-hydroxybenzoate, and vanillate are metabolized to form PCA, which can then be converted to catechol by the action of the PCA decarboxylase for subsequent conversion to muconate.

coumarate, ferulate, 4-hydroxybenzoate, and vanillate (Vardon et al., 2015) as well as from glucose via a 3-dehydroshkimate (3-DHS) dehydratase that converts this intermediate in the shikimate pathway for aromatic amino acid biosynthesis to PCA (Curran et al., 2013; Draths and Frost, 1994; Jung et al., 2015; Niu et al., 2002; Weber et al., 2012). An accumulation of PCA has been observed in strains engineered to produce muconate from aromatic molecules and sugars (Curran et al., 2013; Sonoki et al., 2014; Weber et al., 2012) and is an indication of insufficient PCA decarboxylase activity. The accumulation of intermediates not only reduces the yield and productivity of the engineered biocatalyst, but even trace amounts of residual aromatic compounds can significantly affect the separation of muconate from fermentation broth (Vardon et al., 2016).

Sonoki et al. recently described a means of increasing activity of the PCA decarboxylase that may enable those pursuing strategies to produce muconate via PCA to overcome this bottleneck (Sonoki et al., 2014). Most genes encoding decarboxylases in the hydroxyarylic acid decarboxylase family that includes the PCA decarboxylase, AroY, are co-expressed as an operon with two other small genes shown to be important to activity of the decarboxylase (Lupa et al., 2005; 2008; Matsui et al., 2006). These three genes, *BCD*, are typically clustered in an operon and named for the organism in which they are found (i.e. *Klebsiella pneumoniae* decarboxylase: *kpdB*, *kpdC*, and *kpdD*) with the *C* gene encoding the decarboxylase. While AroY from *Klebsiella pneumoniae* exhibits activity when expressed alone in *Escherichia coli*, Sonoki et al. hypothesized that co-expression of KpdB and/or KpdD, might enhance activity of AroY (Sonoki et al., 2014). Weber and colleagues had previously co-expressed KpdB and KpdD with AroY, but did not compare the PCA decarboxylase activity they achieved with the activity of AroY expressed alone so as to be able to interpret the importance of KpdB and KpdD co-expression (Weber et al., 2012). Sonoki and colleagues found that, in an *Escherichia coli* host, plasmid-based co-expression of KpdB and, in some cases KpdD, enhanced PCA decarboxylase activity relative to expression of AroY alone, essentially eliminating this bottleneck and enhancing production of muconate from vanillin, a lignin-monomer model compound (Sonoki et al., 2014). While the function of B and D proteins were previously unknown, it was recently discovered that homologues of the B protein, UbiX from *E. coli* and PAD1 from *Saccharomyces cerevisiae*, synthesize a novel, prenylated flavin cofactor required for the activity of decarboxylases homologous to the hydroxyarylic acid decarboxylases (Lin et al., 2015; Payne et al., 2015; White et al., 2015). It is likely, then, that KpdB also produces this cofactor, which is required for the decarboxylase activity of AroY.

We previously reported the production of muconate from model lignin monomers as well as alkaline pretreated corn stover by an engineered *P. putida* KT2440 strain (Vardon et al., 2015). This strain utilized the AroY PCA decarboxylase from *Enterobacter cloacae*, which enabled muconate production but also exhibited a substantial accumulation of PCA, similar to that observed by others as described above. In the present study, we sought to apply co-expression of the decarboxylase-associated proteins examined by Sonoki et al. to our system, aiming to improve muconate production. Using genome-integrated gene expression in *P. putida* KT2440-based strains, we demonstrate that co-expression of these

proteins reduces PCA accumulation and enhances muconate production from the lignin monomer *p*-coumarate in both shake flask experiments and fed-batch bioreactor studies. Further, we demonstrate a three-fold improvement in muconate yields from glucose upon co-expression of these proteins. Together, these results suggest that the co-expression of these proteins enhances PCA decarboxylase activity and could enable industrial-scale, biological production of muconic acid from both the lignin and carbohydrate fractions of biomass.

2. Materials and methods

2.1. Plasmid construction

Plasmids for gene replacement were constructed in the vector pCM433 (Addgene plasmid #15670), a gift from Christopher Marx (Marx, 2008). Synthetic ribosome binding sites were designed using the Salis Lab RBS Calculator at salislab.net (Borujeni et al., 2013; Salis et al., 2009). DNA fragments were synthesized by Integrated DNA Technologies (IDT) or SGI-DNA or amplified from *P. putida* genomic DNA using Q5® Hot Start High-Fidelity 2X Master Mix (New England Biolabs) and primers synthesized by IDT. Plasmids were assembled using NEBuilder® HiFi DNA Assembly Master Mix (New England Biolabs) and transformed into NEB® 5-alpha F'I^q competent *E. coli* (New England Biolabs) according to the manufacturer's instructions. Transformants were selected on LB (Lennox) plates containing 10 g/L tryptone, 5 g/L yeast extract, 5 g/L NaCl, and 15 g/L agar, supplemented with either 10 μg/mL tetracycline grown at 37 °C. The sequences of all plasmid inserts were confirmed using Sanger sequencing performed by GENEWIZ, Inc. Specific plasmid construction details, including the sequences of primers and synthesized DNA fragments, can be found in the Supplementary materials and methods.

2.2. Strain construction

Gene replacements were made in *P. putida* KT2440 (ATCC 47054) using the antibiotic/*sacB* method by transforming the suicide integration vector into the target strain by electroporation (Choi et al., 2006), selecting for recombination of the plasmid into the genome on LB (Lennox) plates supplemented with 30 μg/mL tetracycline, and counter-selecting for recombination of the plasmid out of the genome on YT+25% sucrose plates containing 10 g/L yeast extract, 20 g/L tryptone, 250 g/L sucrose, and 18 g/L agar, as described previously (Johnson and Beckham, 2015). Diagnostic colony PCR using MyTaq™ HS Red Mix (Bioline) and primers synthesized by Integrated DNA Technologies was used to confirm gene replacement by amplification of a product of the size expected for the replacement rather than the wild-type sequence. Details on the construction of strains used in this study are provided in the Supplementary Materials and Methods.

2.3. Culture growth and metabolite analysis

For shake flask experiments, 25 mL M9 minimal media (pH 7.2) containing 13.56 g/L Na_2HPO_4, 6 g/L KH_2PO_4, 1 g/L NaCl, 2 g/L NH_4Cl, 2 mM $MgSO_4$, 100 μM $CaCl_2$, and 18 μM $FeSO_4$ supplemented with 4 mM glucose and 20 mM *p*-coumaric acid (Sigma-Aldrich) neutralized with NaOH for strains producing muconate from *p*-coumarate or 50 mM glucose for strains producing muconate from glucose was added to 125 mL baffled flasks. These flasks were inoculated to an optical density at 600 nm (OD_{600}) of 0.1 with cells grown shaking at 225 rpm, 30 °C in LB (Lennox) medium overnight, then centrifuged and resuspended in M9 minimal medium. Flasks were incubated shaking at 225 rpm, 30 °C and sampled periodically to evaluate growth by measurement of the OD_{600} and metabolite concentrations using high performance liquid chromatography (HPLC). Following sampling, an additional 4 mM glucose was added every 6 h for the first 12 h and every 12 h thereafter to cultures producing muconate from *p*-coumarate. Shake flask experiments were performed in triplicate.

Bioreactor experiments were performed in duplicate. Seed cultures were grown in 500 mL baffled flasks containing 100 mL LB (Lennox) medium and incubated shaking at 225 rpm, 30 °C overnight. Cells from these cultures were centrifuged and washed with modified M9 minimal medium with the composition described above except for the substitution of 2.25 g/L $(NH_4)_2SO_4$ instead of 2 g/L NH_4Cl as the nitrogen source and supplementing with 15 mM glucose. These washed cells were used to inoculate 0.5 L BioStat-Q Plus bioreactors (Sartorius Stedim Biotech) containing 300 mL of M9 supplemented with 15 mM glucose, for experiments in which muconate was produced from *p*-coumarate, or 83 mM (15 g/L) glucose, for experiments in which muconate was produced from glucose, to an OD_{600} of 0.2. The pH was maintained at 7.0 by addition of 4 N NaOH. The temperature was controlled at 30 °C, air was sparged at 300 mL/min (1 vvm), and the agitation was set at 350 rpm at the beginning of cultivation.

For fed-batch bioreactor production of muconate from *p*-coumarate, feeding was controlled by saturation of dissolved oxygen (DO-stat). Following inoculation, the agitation was gradually increased from 350 to around 650–700 rpm to maintain an average DO level of ~50%. After 4 h, 1 mM *p*-coumarate was added to the culture. After ~7 h, when the glucose level was close to depletion as indicated by a rapid increase in DO, DO-stat controlled feeding was initiated. When the DO reached 75% feeding solution containing 85 g/L *p*-coumarate, 22.5 g/L glucose, 4.5 g/L $(NH_4)_2SO_4$, and 6 mL/L antifoam 204 (Sigma) was pumped for 30 s intervals (~0.8 mL, bringing the concentration in the bioreactor to 1.3 mM *p*-coumarate and 0.33 mM glucose). Samples were taken periodically to evaluate growth by measurement of the OD_{600}, metabolite concentrations using HPLC for aromatic analytes, and YSI analysis for glucose. These bioreactor experiments were concluded after 73 h.

For fed-batch bioreactor production of muconate from glucose, growth was controlled by the addition of a feeding solution containing 400 g/L glucose and 80 g/L $(NH_4)_2SO_4$. The agitation was manually increased to maintain aerobic conditions (monitored by DO levels) from 350 to 1200 rpm. Samples were taken periodically and glucose measured by YSI analysis. When glucose was close to being depleted, 15 mL of the feeding solution was added with the exception of the fourth (final) feeding, when 30 mL was added. These bioreactor experiments were terminated after 54 h.

HPLC analysis was performed by injecting 6 μL of 0.02 μm filtered culture supernatant onto an Agilent 1100 series system equipped with a Phenomenex Rezex™ RFQ-Fast Acid H+(8%) column and a cation H+guard cartridge (Bio-Rad Laboratories) at 85 °C run using a mobile phase of 0.01 N sulfuric acid at a flow rate of 1.0 mL/min and a diode array detector and refractive index detector for analyte detection. Analytes were identified by comparing retention times and spectral profiles with pure standards. YSI analysis to measure D-glucose in bioreactor experiments was performed using a YSI 7100 MBS (Multiparameter Bioanalytical System, YSI Incorporated).

For shake flask experiments, the standard deviations of the triplicate measurements were calculated using the following equation:

$$\sqrt{\frac{\sum (x-\bar{x})^2}{(n-1)}}$$

in which x is each value in a sample, $\bar{x}$ is the average of the values,

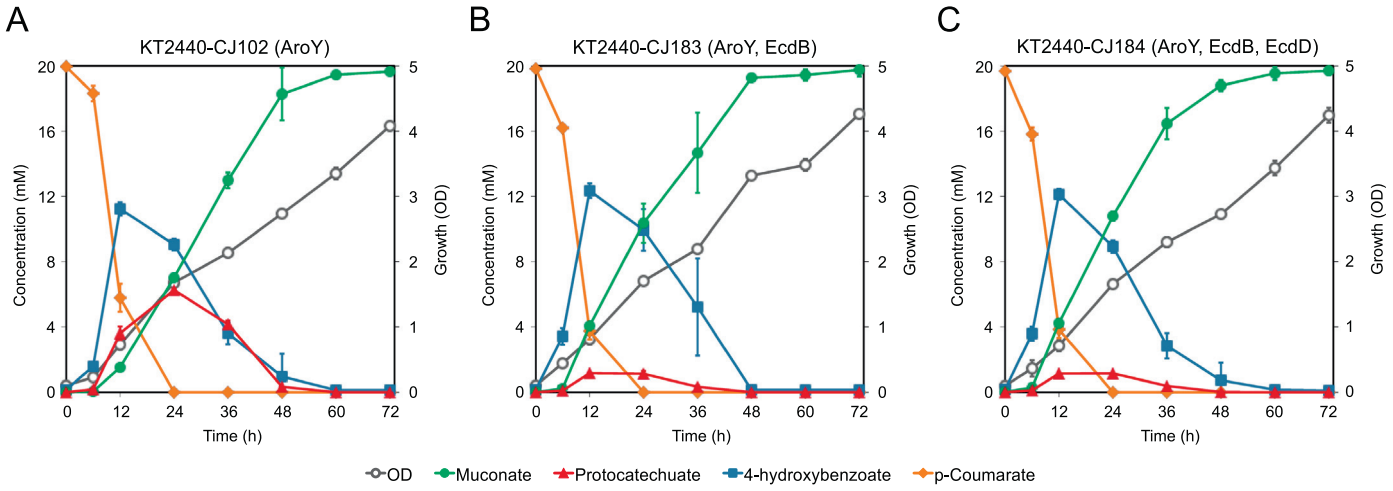

Fig. 2. Shake-flask evaluations of muconate production from *p*-coumarate by engineered *P. putida* KT2440 strains. Cultures were grown in M9 minimal medium containing *p*-coumarate and fed glucose periodically as a source of carbon and energy for growth and sampled to evaluate culture growth by OD_{600} and the concentration of metabolites in the medium by HPLC. Each value represents the average of three biological replicates. The error bars represent standard deviation of the measurements. (A) KT2440-CJ102, expressing the AroY PCA decarboxylase, (B) KT2440-CJ183, expressing AroY as well as EcdB, and (C) KT2440-CJ184, expressing AroY, EcdB, and EcdD.

and n is the number of values.

For bioreactor experiments, the range of duplicate measurements was calculated by subtracting the lowest value from the highest value. Muconate yields were calculated as the ratio of muconic acid production (mM) to *p*-coumaric acid (or glucose) added (mM) into the bioreactor. These calculated values were adjusted to compensate for dilution caused by the addition of NaOH and feeding solution as well as the volume removed for sampling. Muconate productivity (g/L/h) was calculated as the total muconate produced (g/L) during the experiment (h). Specific productivities (g/g cells/h) are expressed as the ratio of muconic acid (g/L) to cells (g/L) at the conclusion of the experiment (h). To calculate the cell biomass (g/L), an experiment to determine the correlation between OD_{600} and cell dry weight was performed and the equation $y=0.4448x+0.1549$ ($R^2=0.989$) describing their relationship was obtained, where y is the cell dry weight in g/L and x is the OD_{600}.

3. Results

We chose *P. putida* KT2440 as the basis of our stain engineering because of its well characterized metabolism (Belda et al., 2016; Chavarría et al., 2013; del Castillo et al., 2007; Jiménez et al., 2010, 2002; Nikel et al., 2015), tolerance to stress such as that induced by aromatic compounds (Nicolaou et al., 2010), and strong potential as an industrial-scale microbial cell factory (Nikel et al., 2014). In *P. putida* KT2440, muconate is generated upon intradiol ring-cleavage of catechol by the paralogous dioxygenases CatA and CatA2 (Fig. 1). The *catA* gene is expressed in the *catRBCA* operon in which the transcriptional regulator CatR drives expression of CatB and CatC, which are responsible for further metabolism of muconate, as well as CatA. We have previously demonstrated that genomic replacement of the *catRBC* genes with the tac promoter, which is constitutively expressed in *P. putida* KT2440, to drive expression of catA (Δ*catRBC*: Ptac:*catA*), results in the accumulation of muconate (Vardon et al., 2015, Vardon et al., 2016). We have also shown that the additional genomic replacement of the *pcaHG* genes, which encode a PCA dioxygenase, with a codon-optimized gene encoding the AroY PCA decarboxylase from *E. cloacae* subsp. *cloacae* ATCC 13047 (Genbank: ADF61496) driven by the tac promoter enabled the production of muconate from the aromatic monomers *p*-coumarate, ferulate, 4-hydroxybenzoate, and vanillate (Vardon et al., 2015, Vardon et al., 2016). In order to evaluate the effect of co-expression of these decarboxylase-associated proteins in our system, we first identified their *Enterobacter cloacae* homologues. EcdB (Genbank: ADF63617), named based on convention after the abbreviation of *Enterobacter cloacae* decarboxylase, is 89.3% identical to KpdB used by Sonoki et al. while EcdD (Genbank: ADF63615) is 94.5% identical to KpdD. We then constructed strains in which codon-optimized genes encoding EcdB alone or EcdB and EcdD were integrated in the *pcaHG* locus downstream of the tac promoter driven gene encoding AroY. Co-expression of the D protein with AroY in the absence of B protein was not examined because this combination was shown previously to attenuate PCA decarboxylase activity (Sonoki et al., 2014).

To determine if these proteins enhance PCA decarboxylase activity when expressed from genes integrated as single copies in the genome, these three strains, KT2440-CJ102 (Δ*pcaHG*::Ptac:*aroY*), KT2440-CJ183 (Δ*pcaHG*::Ptac:*aroY*:*ecdB*), and KT2440-CJ184 (Δ*pcaHG*::Ptac:*aroY*:*ecdB*:*ecdD*) were evaluated in shake-flask experiments for production of muconate from 20 mM *p*-coumarate, one of the predominant aromatic lignin-monomers produced from alkaline pretreatment of corn stover and switchgrass (Karp et al., 2014; 2015; Vardon et al., 2015) in M9 minimal medium using glucose (4 mM fed every 6 h for the first 12 h and every 12 h thereafter) as a carbon source for growth and energy. As observed previously, expression of AroY alone in KT2440-CJ102 enabled the production of muconate from *p*-coumarate, but the productivity was affected by a substantial accumulation of PCA, up to 6.3 mM at 24 h (Fig. 2A). Upon co-expression of EcdB alone (KT2440-CJ183, Fig. 2B) or EcdB and EcdD (KT2440-CJ184, Fig. 2C), PCA only accumulated to 1.2 mM, peaking at 12 h in both cases, resulting in an increase in productivity between 6 and 36 h. These results clearly demonstrate that the benefit of co-expressing these proteins along with AroY can be applied to a genome-integrated host with potential as an industrially-relevant biocatalyst.

We next sought to determine if the benefit of co-expressing EcdB and EcdD also applies to more industrially relevant fed-batch bioreactor cultivation. We used a DO-stat strategy in which small pulses of a solution containing 85 g/L *p*-coumarate and 22.5 g/L glucose (corresponding to 1.3 mM and 0.3 mM in the bioreactor) were fed when the DO increased to a preset value (75%), indicating that the glucose from the previous pulse had been consumed. This enabled us to avoid the accumulation of glucose, which could

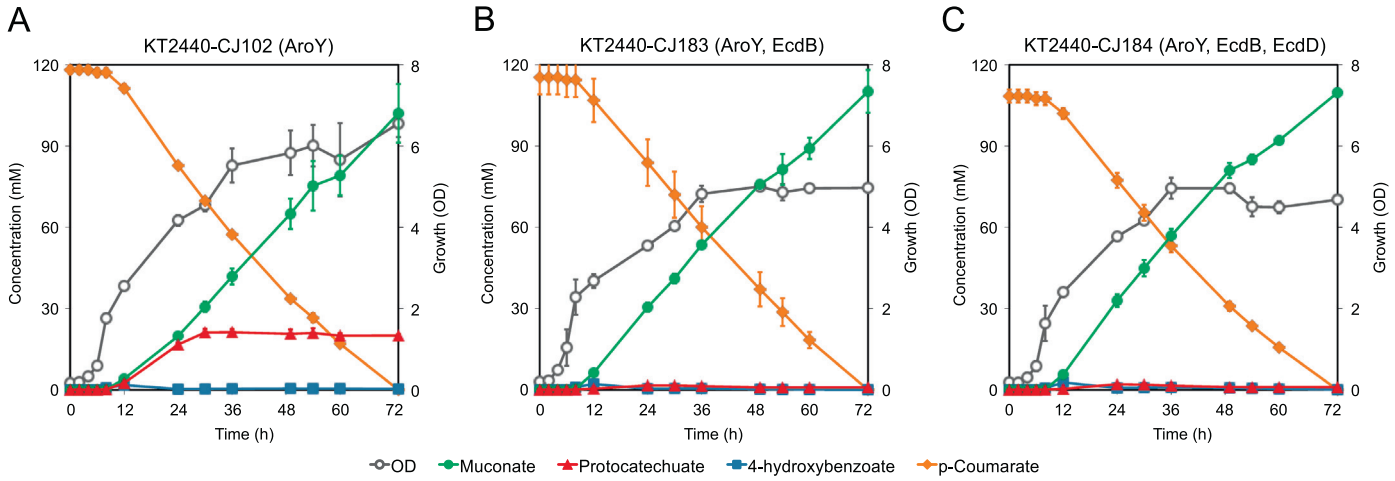

Fig. 3. Bioreactor evaluations of muconate production from *p*-coumarate by engineered *P. putida* KT2440 strains. Cultures were grown for 72 h in M9 minimal medium by DO-stat control, pulsing *p*-coumarate and glucose to reach bioreactor concentrations of 1.3 mM and 0.33 mM, respectively. Cultures were sampled to evaluate bacterial growth by OD_{600} and the concentration of metabolites in the medium by HPLC. *p*-Coumarate values graphed above represent the amount remaining of the total *p*-coumarate fed by the conclusion of the experiment. Each value represents the average of two biological replicates. The error bars represent the range of the measurements. (A) KT2440-CJ102, expressing the AroY PCA decarboxylase, (B) KT2440-CJ183, expressing AroY as well as EcdB, and (C) KT2440-CJ184, expressing AroY, EcdB, and EcdD.

Table 1
Parameters at 73 h from bioreactor experiments to produce muconate from *p*-coumarate. Values represent the average and range of biological duplicates.

Strain	Genotype	Titer (g/L)	Yield (M/M)	Productivity (g/L/h)	Specific productivity (mg/g cells[a]/h)
KT2440-CJ102	*P. putida* KT2440 Δ*catRBC*::Ptac:*catA* Δ*pcaHG*::Ptac:*aroY*	14.50 ± 1.54	0.86 ± 0.08	0.20 ± 0.02	64.55 ± 3.77
KT2440-CJ183	*P. putida* KT2440 Δ*catRBC*::Ptac:*catA* Δ*pcaHG*::Ptac:*aroY*:*ecdB*	15.65 ± 1.12	0.95 ± 0.02	0.21 ± 0.02	90.57 ± 5.28
KT2440-CJ184	*P. putida* KT2440 Δ*catRBC*::Ptac:*catA* Δ*pcaHG*::Ptac:*aroY*:*ecdB*:*ecdD*	15.59 ± 0.01	1.01 ± 0.02	0.21 ± 0.00	95.46 ± 0.47

[a] Cell dry weights inferred based on correlation with OD_{600} as described in materials and methods.

trigger catabolite repression that might affect aromatic metabolism (Rojo, 2010), as well as the accumulation of *p*-coumarate, which is toxic at concentrations > 15 g/L (data not shown). Using this strategy, muconate production by KT2440-CJ102, KT2440-CJ183, and KT2440-CJ184 were compared. As we observed in the shake flask experiments, KT2440-CJ102 exhibited an accumulation of PCA (Fig. 3A) that diminished upon co-expression of EcdB in KT2440-CJ183 (Fig. 3B) or EcdB and EcdD in KT2440-CJ184 (Fig. 3C), leading to a trend toward increases in the final muconate titer, yield, and productivity after 73 h (Table 1). Importantly, KT2440-CJ102 achieved a specific productivity (mg muconate/g cells/h) of 64.55 ± 3.77 while KT2440-CJ183 and KT2440-CJ184 achieved specific productivities of 90.57 ± 5.28 and 95.46 ± 0.47, respectively. Thus, co-expression of EcdB and EcdD with AroY reduces the accumulation of PCA and increases muconate production during fed-batch bioreactor cultivations producing much higher titers of muconate than those observed in shake flask experiments, up to 15.59 ± 0.01 g/L with KT2440-CJ184.

As mentioned above, conversion of PCA to catechol is also central to pathways for production of muconate from sugars via

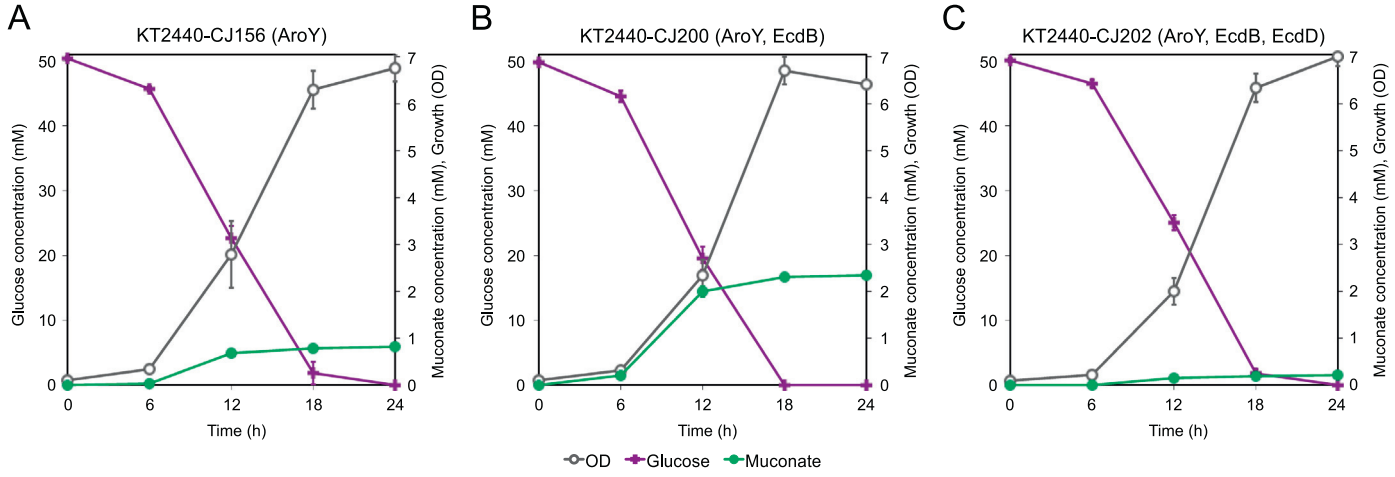

Fig. 4. Shake-flask evaluations of muconate production from glucose by engineered *P. putida* KT2440 strains. Cultures were grown for 24 h in M9 minimal medium containing glucose for conversion to muconate and as a source of carbon and energy for growth and sampled to evaluate culture growth by OD_{600} and the concentration of metabolites in the medium by HPLC. Each value represents the average of three biological replicates. The error bars represent standard deviation of the measurements. (A) KT2440-CJ156, expressing the AroY PCA decarboxylase, (B) KT2440-CJ200, expressing AroY as well as EcdB, and (C) KT2440-CJ202, expressing AroY, EcdB, and EcdD.

3-DHS, an intermediate in the shikimate pathways for aromatic amino acid synthesis. As such, we next set out to determine how enhancing PCA activity by co-expression of EcdB or EcdB and EcdD along with AroY might benefit the production of muconate from glucose. In order to convert glucose to muconate, we constructed strains similar to those described above for production of muconate from aromatic lignin-monomers but that also incorporated a codon optimized gene encoding AsbF, a 3-DHS dehydratase from *Bacillus cereus* ATCC 14579 (Genbank: AAP08954) that converts 3-DHS to PCA (Fox et al., 2008). We then performed a shake flask experiment comparing KT2440-CJ156 (Δ*pcaHG*::Ptac:*aroY*:*asbF*), KT2440-CJ200 (Δ*pcaHG*::Ptac:*aroY*:*ecdB*:*asbF*), and KT2440-CJ202 (Δ*pcaHG*::Ptac:*aroY*:*ecdB*:*ecdD*:*asbF*) grow in M9 minimal medium contain 50 mM glucose. KT2440-CJ156 produced 0.8 mM muconate, a 1.6% yield (mol/mol) from 50 mM glucose (Fig. 4A), indicating that AsbF is functional and enables production of muconate from glucose. The addition of EcdB in CJ200 resulted in an almost three-fold improvement in muconate titer, producing 2.3 mM muconate, a 4.7% yield (mol/mol) (Fig. 4B). Interestingly, KT2440-CJ202, which expresses EcdD in addition to EcdB and AroY, produced only 0.2 mM muconate (Fig. 4C), less than KT2440-CJ156 expressing AroY alone (Fig. 4A). To confirm that this result was not caused by some unknown mutation or other stochastic difference in this strain, we repeated this experiment with a second strain that was constructed identically to KT2440-CJ202 but this strain exhibited the same low muconate yield (data not shown). These results demonstrate that increased PCA decarboxylase activity resulting from co-expression of EcdB greatly enhances muconate production from sugars, which is attenuated by the additional expression of EcdD.

As before, we next evaluated these strains in bioreactor cultivations. The production of muconate from glucose alone eliminated the need for the DO-stat control strategy used in our previous bioreactor experiments in order to avoid possible catabolite repression and toxicity of aromatic substrates. Instead, the cultures were fed an initial 15 g/L of glucose and when the glucose was almost depleted the culture was fed another 15 g/L of glucose. These feedings were repeated twice more along with a single, final feeding of 30 g/L glucose (Fig. 5). After 54 h, KT2440-CJ156, produced only 1.44 ± 0.14 g/L muconate (Fig. 5A) while KT2440-CJ200, with its additional expression of EcdB, produced 4.92 ± 0.48 g/L (Fig. 5B) and achieved a yield, productivity, and specific productivity that were at least three-fold greater than those of KT2440-CJ156 (Table 2). As observed in the shake flask experiments performed using these strains, the additional expression of EcdD reduced the production of muconate (Fig. 5C), even relative to KT2440-CJ156 expressing AroY alone (Fig. 5A).

4. Discussion and conclusions

In this study, we have clearly demonstrated that co-expression of EcdB and EcdD reduces the accumulation of PCA in *P. putida* KT2440-based strains engineered using genome-integrated gene expression to produce muconate from aromatic molecules in shake flask (Fig. 2) and bioreactor (Fig. 3) cultivations. In addition to the obvious effect upon product yields, reducing the accumulation of an aromatic intermediate such as protocatechuate could substantially reduce costs associated with separation of the final product by reducing the required loading of activated carbon for removal of residual aromatic compounds (Vardon et al., 2016). We have also demonstrated that expression of EcdB increased muconate production by about 3-fold in strains engineered to produce muconate from glucose, both in shake flask (Fig. 4) and bioreactor experiments (Fig. 5). The maximum titer (4.92 ± 0.48 g/L) and yield (0.077 ± 0.005 mol/mol) of muconate from glucose reported here (Table 2) are nearly an order of magnitude higher than those described in yeast-based systems (Curran et al., 2013; Weber et al., 2012), but considerably lower than those reported in *E. coli* host systems (Draths and Frost, 1994; Niu et al., 2002). All of these previously described systems, however, relied on plasmid-based gene expression and, in most cases, the introduction of mutations that required cultures to be supplemented with aromatic amino acids, both of which are generally inconsistent with at-scale production processes. As such, it is important to note that the *P. putida* KT2440-based strains described here represent the only reported system for production of muconate from glucose by strains engineered using entirely genome-integrated gene expression, without the requirement of costly amino acid supplementation. Additional metabolic engineering to increase the flux of carbon to muconate will undoubtedly be of benefit to the "base case" strains described here and will be necessary to achieve industrially-relevant levels of production; this work is ongoing in our laboratory currently.

In shake flask experiments, co-expression of EcdB or EcdB and EcdD also had the unexpected benefit of increasing the rate of

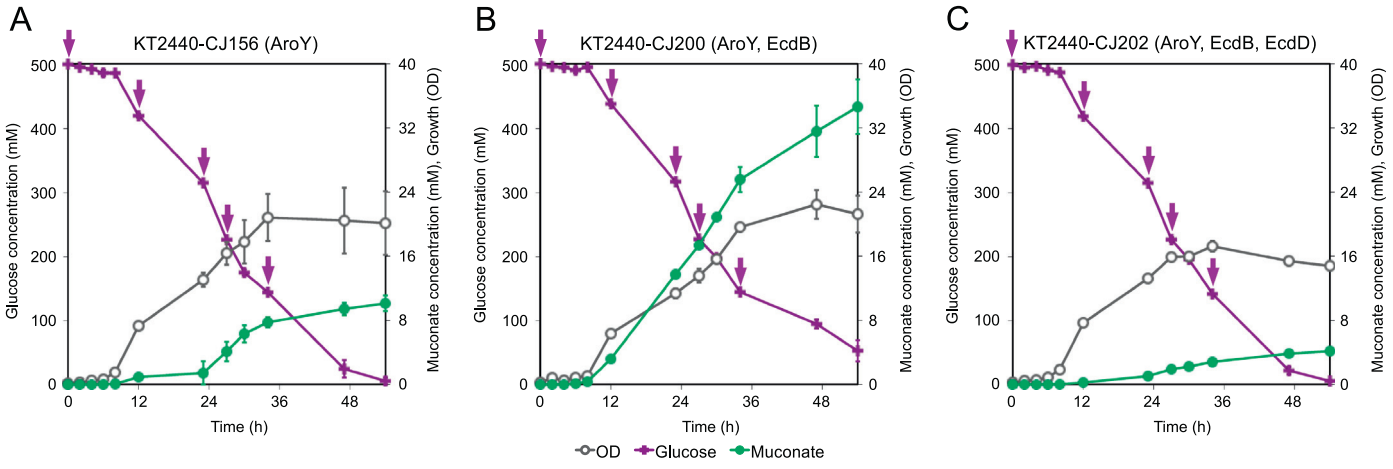

Fig. 5. Bioreactor evaluations of muconate production from glucose by engineered *P. putida* KT2440 strains. Cultures were grown in M9 minimal medium and fed glucose at time points as indicated by arrows. Cultures were sampled to evaluate culture growth by OD_{600} and the concentration of metabolites in the medium by HPLC. Glucose values graphed above represent the amount remaining of the total glucose fed by the conclusion of the experiment. Each value represents the average of two biological replicates. The error bars represent the range of the measurements. (A) KT2440-CJ156, expressing the AroY PCA decarboxylase, (B) KT2440-CJ200, expressing AroY as well as EcdB, and (C) KT2440-CJ202, expressing AroY, EcdB, and EcdD.

Table 2
Parameters at 54 h from bioreactor experiments to produce muconate from glucose. Values represent the average and range of biological duplicates.

Strain	Genotype	Titer (g/L)	Yield (M/M)	Productivity (g/L/h)	Specific productivity (mg/g cells[a]/h)
KT2440-CJ156	*P. putida* KT2440 Δ*catRBC*::Ptac:*catA* Δ*pcaHG*::Ptac:*aroY*:*asbF*	1.44 ± 0.14	0.021 ± 0.002	0.03 ± 0.00	3.10 ± 0.89
KT2440-CJ200	*P. putida* KT2440 Δ*catRBC*: :Ptac:*catA* Δ*pcaHG*: :Ptac:*aroY*:*ecdB*:*asbF*	4.92 ± 0.48	0.077 ± 0.005	0.09 ± 0.01	9.50 ± 0.08
KT2240-CJ202	*P. putida* KT2440 Δ*catRBC*: :Ptac:*catA* Δ*pcaHG*: :Ptac:*aroY*:*ecdB*:*ecdD*:*asbF*	0.59 ± 0.03	0.008 ± 0.001	0.01 ± 0.00	1.63 ± 0.11

[a] Cell dry weights inferred based on correlation with OD_{600} as described in materials and methods.

catabolism of *p*-coumarate (Fig. 2B and 2C vs. 2A), though this ultimately resulted in greater accumulation of 4-hydroxybenzoate. Based on the data from these shake flask experiments, the accumulation of 4-hydroxybenzoate appears to represent a substantial bottleneck in the pathway to muconate. In the corresponding bioreactor experiments (Fig. 3), however, a substantial accumulation of 4-hydroxybenzoate was not observed. Conversely, however, these bioreactor cultures exhibited lower growth rates once feeding of *p*-coumarate was initiated relative to the strain expressing AroY alone (Fig. 3B and 3C vs. 3A), which were not observed in shake flask experiments. This might be associated with the increased accumulation of muconate, which could be inhibitory. Further experiments will be required to determine if this can be overcome with additional optimization of bioreactor conditions or the strains themselves. The differences in performance of these strains under different growth conditions underscores the importance of evaluating strains in the controlled environment of a bioreactor.

Efforts to understand the mechanism whereby the expression of EcdB modulates the activity of the AroY PCA decarboxylase may be informed by an examination of the function of its homologues. Decarboxylases in the hydroxyarylic acid decarboxylase family, which includes AroY and the C proteins discussed in the introduction, are homologous to UbiD, a bacterial 3-octaprenyl-4-hydroxy-benzoate decarboxylase required for biosynthesis of ubiquinone (coenzyme Q), and the ferulic acid decarboxylase (FDC) from *Saccharomyces cerevisiae* (Lupa et al., 2005; White et al., 2015). The *B* genes usually co-expressed with the decarboxylase *C* genes are homologous to the bacterial *ubiX* and yeast *PAD1* genes that were recently shown to encode a flavin prenyltransferase responsible for producing a prenylated-FMN cofactor required by UbiD and FDC (Lin et al., 2015; Payne et al., 2015; White et al., 2015). It is likely, then, that the B proteins produce the same specialized cofactor that is utilized by the C decarboxylases as well as AroY. This would explain why AroY is active when expressed without the B protein in *E. coli*, in which the prenylated-FMN is already produced by UbiX, or *S. cerevisiae* (Curran et al., 2013), where it is produced by PAD1. PCA decarboxylase activity is enhanced by co-expression of the B protein in *E. coli* (Sonoki et al., 2014), probably by increasing production of prenylated-FMN beyond what is synthesized by the native UbiX alone, which is apparently insufficient to also support full activity of the heterologously expressed AroY. This likely also applies to expression of AroY in *P. putida* KT2440, which also natively expresses a UbiX homologue (PP_0548, Genbank: NP_742711.1).

The role of the D protein, which shows no homology to any proteins characterized to date, remains elusive. We have shown that co-expression of *ecdD* with *ecdB* and *aroY* provides a slight, but consistent reduction in accumulated PCA and improvement in muconate production relative to expression of only *ecdB* and *aroY* in strains engineered to produce muconate from aromatic lignin monomers (Figs. 2 and 3, Table 1.). However, in strains engineered to produce muconate from glucose by the incorporation of the DHS dehydratase, AsbF, its expression attenuates muconate production below that observed by expression of AroY alone (Figs. 4 and 5, Table 2). Sonoki and colleagues observed similarly inconsistent results with expression of *kpdD* in their *E. coli* host; when *aroY* was expressed on one plasmid and *kpdB* and *kpdD* were expressed on a second plasmid, it resulted in greater PCA decarboxylase activity than when the second plasmid expressed only *kpdB*. When all of these genes were expressed on a single plasmid, however, the addition of *kpdD* reduced decarboxylase activity relative to the plasmid expressing only *aroY* and *kpdB* (Sonoki et al., 2014). Taken together, these results suggest that the effect of the D protein on the PCA decarboxylase activity of AroY and the B protein is highly context dependent. While in the study by Sonoki et al., differing effects were seen in cases where *kpdD* may have been expressed at very different levels relative to *aroY*, our *P. putida* KT2440-derived strains KT2440-CJ184 and KT2400-CJ202 only differ in that the *asbF* gene was incorporated in the synthetic operon integrated into the genome of KT2440-CJ202 (Ptac:*aroY*:*ecdB*:*ecdD*:*asbF*), in which the activity of the PCA decarboxylase was attenuated by co-expression of EcdD, but not in that of KT2440-CJ184 (Ptac:*aroY*:*ecdB*:*ecdD*), in which EcdD co-expression enhanced its activity. We believe it is unlikely that the *asbF* gene, which was incorporated at the 5′ end of the operon, would affect expression of *ecdD* upstream of it, but it is still formally possible that expression of *ecdD* is affected by the addition of *asbF*. It is also formally possible that AsbF and EcdD interact in a way that affects the function of EcdD. Because the benefit of co-expressing the *D* gene on PCA decarboxylase activity is negligible at best and has the potential to be deleterious based on our findings and those of Sonoki and colleagues, it is tempting, and even advisable, to forgo its inclusion in metabolic engineering strategies that incorporate the PCA decarboxylase. Its evolutionary conservation, coupled with our findings and those of Sonoki et al. (Sonoki et al., 2014) demonstrating that it can enhance PCA decarboxylase in certain circumstances, may justify greater examination of this protein.

The PCA decarboxylase itself is certainly worthy of further investigation. While molecules such as 4-hydroxybenzoate and vanillate, which are generated by relatively mild lignin depolymerization methods (Linger et al., 2014; Salvachúa et al., 2015) are metabolized through PCA, their decarboxylated counterparts, phenol and guaiacol, less substituted products arising from harsher lignin depolymerization methods (Katahira et al., 2016; Kruger et al., 2016), are metabolized through catechol. Decarboxylases capable of catalyzing these reactions have been characterized and demonstrated to, technically if not efficiently, catalyze the reverse reaction (carboxylation) as well (Chow et al., 1999; Lupa et al., 2008; 2005), as has the PCA decarboxylase (He and Wiegel, 1996; Yoshida at al., 2010). Thus, AroY and these other hydroxyarylic acid decarboxylases can essentially bridge the PCA and catechol branches of the β-ketoadipate pathway as well as the upper pathways that funnel into them, a capability that is likely to become important as interest grows in metabolic engineering aimed at lignin valorization (Beckham et al., 2016).

Acknowledgements

We thank the US Department of Energy Bioenergy Technologies Office (DOE-BETO) for funding the lignin portion of this work via Contract No. DE-AC36-08GO28308 with the National Renewable Energy Laboratory, and the National Renewable Energy Laboratory Directed Research and Development for funding the sugar conversion portion of this work. We thank Eduardo Diaz for helpful discussions related to the function of EcdB, Mary Ann Franden for information regarding the toxicity of *p*-coumarate, and Ryan Spiller for bioreactor setup.

Appendix A. Supplementary material

Supplementary data associated with this article can be found in the online version at http://dx.doi.org/10.1016/j.meteno.2016.04.002.

References

Beckham, G.T., Johnson, C.W., Karp, E.M., Salvachúa, D., Vardon, D.R., 2016. Opportunities and challenges in biological lignin valorization. Curr. Opin. Biotechnol. 42, 40–53. http://dx.doi.org/10.1016/j.copbio.2016.02.030.

Belda, E., van Heck, R.G.A., Lopez-Sanchez, M.J., Cruveiller, S., Barbe, V., Fraser, C., Klenk, H.-P., Petersen, J., Morgat, A., Nikel, P.I., Vallenet, D., Rouy, Z., Sekowska, A., Martins dos Santos, V.A.P., de Lorenzo, V., Danchin, A., Médigue, C., 2016. The revisited genome of Pseudomonas putida KT2440 enlightens its value as a robust metabolic chassis. Environ. Microbiol. . http://dx.doi.org/10.1111/1462–2920.13230

Borujeni, A.E., Channarasappa, A.S., Salis, H.M., 2013. Translation rate is controlled by coupled trade-offs between site accessibility, selective RNA unfolding and sliding at upstream standby sites. Nucleic Acids . http://dx.doi.org/10.1093/nar/gkt1139/-/DC1.

Chavarría, M., Nikel, P.I., Pérez-Pantoja, D., de Lorenzo, V., 2013. The Entner-Doudoroff pathway empowers Pseudomonas putida KT2440 with a high tolerance to oxidative stress. Environ. Microbiol. 15, 1772–1785. http://dx.doi.org/10.1111/1462–2920.12069.

Choi, K.-H., Kumar, A., Schweizer, H.P., 2006. A 10-min method for preparation of highly electrocompetent Pseudomonas aeruginosa cells: Application for DNA fragment transfer between chromosomes and plasmid transformation. J. Microbiol. Methods 64, 391–397. http://dx.doi.org/10.1016/j.mimet.2005.06.001.

Chow, K.T., Pope, M.K., Davies, J., 1999. Characterization of a vanillic acid non-oxidative decarboxylation gene cluster from Streptomyces sp. D7. Microbiology 145, 2393–2403.

Curran, K.A., Leavitt, J.M., Karim, A.S., Alper, H.S., 2013. Metabolic engineering of muconic acid production in Saccharomyces cerevisiae. Metab. Eng. 15, 55–66. http://dx.doi.org/10.1016/j.ymben.2012.10.003.

del Castillo, T., Ramos, J.L., Rodriguez-Herva, J.J., Fuhrer, T., Sauer, U., Duque, E., 2007. Convergent peripheral pathways catalyze initial glucose catabolism in pseudomonas putida: genomic and flux analysis. J. Bacteriol. 189, 5142–5152. http://dx.doi.org/10.1128/JB.00203–07.

Deng, Y., Ma, L., Mao, Y., 2016. Biological production of adipic acid from renewable substrates: Current and future methods. Biochem. Eng. J. 105, 16–26. http://dx.doi.org/10.1016/j.bej.2015.08.015.

Draths, K.M., Frost, J.W., 1994. Environmentally compatible synthesis of adipic acid from D-glucose. J. Am. Chem. Soc. 116, 399–400.

Fox, D.T., Hotta, K., Kim, C.-Y., Koppisch, A.T., 2008. The Missing Link in Petrobactin Biosynthesis: asbF Encodes a (−)-3-Dehydroshikimate Dehydratase. Biochemistry 47, 12251–12253. http://dx.doi.org/:10.1021/bi801876q.

Harwood, C.S., Parales, R.E., 1996. The beta-ketoadipate pathway and the biology of self-identity. Annu. Rev. Microbiol. 50, 553–590. http://dx.doi.org/10.1146/annurev.micro.50.1.553.

He, Z., Wiegel, J., 1996. Purification and characterization of an oxygen-sensitive, reversible 3,4-dihydroxybenzoate decarboxylase from Clostridium hydroxybenzoicum. J. Bacteriol. 178, 3539–3543.

Jiménez, J.I., Nogales, J., García, J.L., Díaz, E., 2010. A Genomic View of the Catabolism of Aromatic Compounds in Pseudomonas, in: Handbook of Hydrocarbon and Lipid Microbiology. Springer Berlin Heidelberg, Berlin, Heidelberg, pp. 1297–1325. doi:10.1007/978–3-540–77587–4_91.

Jiménez, J.I., Miñambres, B., García, J.L., Díaz, E., 2002. Genomic analysis of the aromatic catabolic pathways from Pseudomonas putida KT2440. Environ. Microbiol. 4, 824–841.

Johnson, C.W., Beckham, G.T., 2015. Aromatic catabolic pathway selection for optimal production of pyruvate and lactate from lignin. Metab. Eng. 28, 240–247. http://dx.doi.org/10.1016/j.ymben.2015.01.005.

Jung, H.-M., Jung, M.-Y., Oh, M.-K., 2015. Metabolic engineering of Klebsiella pneumoniae for the production of cis,cis-muconic acid. Appl. Microbiol. Biotechnol. . http://dx.doi.org/10.1007/s00253–015–6442–3

Karp, E.M., Donohoe, B.S., O'Brien, M.H., Ciesielski, P.N., Mittal, A., Biddy, M.J., Beckham, G.T., 2014. Alkaline Pretreatment of Corn Stover: Bench-Scale Fractionation and Stream Characterization. ACS Sustain. Chem. Eng. 2, 1481–1491. http://dx.doi.org/10.1021/sc500126u.

Karp, E.M., Resch, M.G., Donohoe, B.S., Ciesielski, P.N., O'Brien, M.H., Nill, J.E., Mittal, A., Biddy, M.J., Beckham, G.T., 2015. Alkaline pretreatment of switchgrass. ACS Sustain. Chem. Eng. 3, 1479–1491. http://dx.doi.org/10.1021/acssuschemeng.5b00201.

Katahira, R., Mittal, A., McKinney, K., Chen, X., 2016. Base-catalyzed depolymerization of biorefinery lignins. ACS Sustain Chem. Eng. 5, b01451. http://dx.doi.org/10.1021/acssuschemeng.5b01451.

Kruger, J.S., Cleveland, N.S., Zhang, S., Katahira, R., Black, B.A., Chupka, G.M., Lammens, T., Hamilton, P.G., Biddy, M.J., Beckham, G.T., 2016. Lignin Depolymerization with Nitrate-Intercalated Hydrotalcite. Catal. ACS Catal., 1316–1328. http://dx.doi.org/10.1021/acscatal.5b02062.

Lin, F., Ferguson, K.L., Boyer, D.R., Lin, X.N., Marsh, E.N.G., 2015. Isofunctional Enzymes PAD1 and UbiX Catalyze Formation of a Novel Cofactor Required by Ferulic Acid Decarboxylase and 4-Hydroxy-3-polyprenylbenzoic Acid Decarboxylase. ACS Chem. Biol. 10, 1137–1144. doi:10.1021/cb5008103.

Linger, J.G., Vardon, D.R., Guarnieri, M.T., Karp, E.M., Hunsinger, G.B., Franden, M.A., Johnson, C.W., Chupka, G., Strathmann, T.J., Pienkos, P.T., Beckham, G.T., 2014. Lignin valorization through integrated biological funneling and chemical catalysis. Proceedings of the National Academy of Sciences 111, 12013–12018. doi:10.1073/pnas.1410657111.

Lu, R., Lu, F., Chen, J., Yu, W., Huang, Q., Zhang, J., Xu, J., 2015. Production of diethyl terephthalate from biomass-derived muconic acid. Angew. Chem. Int. Ed. 55, 249–253. http://dx.doi.org/10.1002/anie.201509149.

Lupa, B., Lyon, D., Gibbs, M.D., Reeves, R.A., Wiegel, J., 2005. Distribution of genes encoding the microbial non-oxidative reversible hydroxyarylic acid decarboxylases/phenol carboxylases. Genomics 86, 342–351. http://dx.doi.org/10.1016/j.ygeno.2005.05.002.

Lupa, B., Lyon, D., Shaw, L.N., Sieprawska-Lupa, M., Wiegel, J., 2008. Properties of the reversible nonoxidative vanillate /4-hydroxybenzoate decarboxylase from Bacillus subtilis. Can. J. Microbiol. 54, 75–81. http://dx.doi.org/10.1139/W07–113.

Marx, C.J., 2008. Development of a broad-host-range sacB-based vector for unmarked allelic exchange. BMC Res. Notes 1, 1. http://dx.doi.org/10.1186/1756–0500–1-1.

Matsui, T., Yoshida, T., Hayashi, T., Nagasawa, T., 2006. Purification, characterization, and gene cloning of 4-hydroxybenzoate decarboxylase of Enterobacter cloacae P240. Arch. Microbiol. 186, 21–29. http://dx.doi.org/10.1007/s00203–006–0117–5.

Nicolaou, S.A., Gaida, S.M., Papoutsakis, E.T., 2010. A comparative view of metabolite and substrate stress and tolerance in microbial bioprocessing From biofuels and chemicals, to biocatalysis and bioremediation. Metab. Eng. 12, 307–331. http://dx.doi.org/10.1016/j.ymben.2010.03.004.

Nikel, P.I., Chavarría, M., Fuhrer, T., Sauer, U., de Lorenzo, V., 2015. Pseudomonas putida KT2440 strain metabolizes glucose through a cycle formed by enzymes of the entner-doudoroff, embden-meyerhof-parnas, and pentose phosphate pathways. J. Biol. Chem. 290, 25920–25932. http://dx.doi.org/10.1074/jbc.M115.687749.

Nikel, P.I., Martínez-García, E., de Lorenzo, V., 2014. Biotechnological domestication of pseudomonads using synthetic biology. Nat. Rev. Microbiol. 12, 368–379. http://dx.doi.org/10.1038/nrmicro3253.

Niu, W., Draths, K.M., Frost, J.W., 2002. Benzene-free synthesis of adipic acid. Biotechnol. Prog. 18, 201–211. http://dx.doi.org/10.1021/bp010179x.

Ornston, L.N., Stanier, R.Y., 1966. The conversion of catechol and protocatechuate to beta-ketoadipate by Pseudomonas putida. J. Biol. Chem. 241, 3776–3786.

Payne, K.A.P., White, M.D., Fisher, K., Khara, B., Bailey, S.S., Parker, D., Rattray, N.J.W., Trivedi, D.K., Goodacre, R., Beveridge, R., Barran, P., Rigby, S.E.J., Scrutton, N.S., Hay, S., Leys, D., 2015. New cofactor supports α,β-unsaturated acid decarboxylation via 1,3-dipolar cycloaddition. Nature 522, 497–501. http://dx.doi.org/10.1038/nature14560.

Polen, T., Spelberg, M., Bott, M., 2013. Toward biotechnological production of adipic acid and precursors from biorenewables. J. Biotechnol. 167, 75–84. http://dx.doi.org/10.1016/j.jbiotec.2012.07.008.

Rojo, F., 2010. Carbon catabolite repression in Pseudomonas: optimizing metabolic versatility and interactions with the environment. FEMS Microbiol. Rev., 1–27. http://dx.doi.org/10.1111/j.1574–6976.2010.00218.x.

Salis, H.M., Mirsky, E.A., Voigt, C.A., 2009. Automated design of synthetic ribosome binding sites to control protein expression. Nat. Publ. Group 27, 946–950. http://dx.doi.org/10.1038/nbt.1568.

Salvachúa, D., Karp, E.M., Nimlos, C.T., Vardon, D.R., Beckham, G.T., 2015. Towards lignin consolidated bioprocessing: simultaneous lignin depolymerization and product generation by bacteria. Green Chem. 17, 4951–4967. http://dx.doi.org/10.1039/C5GC01165E.

Sonoki, T., Morooka, M., Sakamoto, K., Otsuka, Y., Nakamura, M., Jellison, J., Goodell, B., 2014. Enhancement of protocatechuate decarboxylase activity for the effective production of muconate from lignin-related aromatic compounds. J. Biotechnol. 192, 71–77. http://dx.doi.org/10.1016/j.jbiotec.2014.10.027.

Van de Vyver, S., Román-Leshkov, Y., 2013. Emerging catalytic processes for the production of adipic acid. Catal. Sci. Technol. 3, 1465–1479. http://dx.doi.org/10.1039/C3CY20728E.

Vardon, D.R., Franden, M.A., Johnson, C.W., Karp, E.M., Guarnieri, M.T., Linger, J.G., Salm, M.J., Strathmann, T.J., Beckham, G.T., 2015. Adipic acid production from lignin. Energy Environ. Sci. 8, 617–628. http://dx.doi.org/10.1039/C4EE03230F.

Vardon, D.R., Rorrer, N.A., Salvachúa, D., Settle, A.E., Johnson, C.W., Menart, M.J., Cleveland, N.S., Ciesielski, P.N., Steirer, K.X., Dorgan, J.R., Beckham, G.T., 2016. cis,cis-Muconic acid: separation and catalysis to bio-adipic acid for nylon-6,6 polymerization. Green. Chem., 1–17. http://dx.doi.org/10.1039/C5GC02844B.

Weber, C., Brückner, C., Weinreb, S., Lehr, C., Essl, C., Boles, E., 2012. Biosynthesis of cis,cis-muconic acid and its aromatic precursors, catechol and protocatechuic acid, from renewable feedstocks by Saccharomyces cerevisiae. Appl. Environ. Microbiol. 78, 8421–8430. http://dx.doi.org/10.1128/AEM.01983–12.

White, M.D., Payne, K.A.P., Fisher, K., Marshall, S.A., Parker, D., Rattray, N.J.W., Trivedi, D.K., Goodacre, R., Rigby, S.E.J., Scrutton, N.S., Hay, S., Leys, D., 2015. UbiX is a flavin prenyltransferase required for bacterial ubiquinone biosynthesis. Nature 522, 502–506. http://dx.doi.org/10.1038/nature14559.

Xie, N.-Z., Liang, H., Huang, R.-B., Xu, P., 2014. Biotechnological production of muconic acid: current status and future prospects. Biotechnol. Adv. 32, 615–622. http://dx.doi.org/10.1016/j.biotechadv.2014.04.001.

Yoshida, T., Inami, Y., Matsui, T., Nagasawa, T., 2010. Regioselective carboxylation of catechol by 3,4-dihydroxybenzoate decarboxylase of Enterobacter cloacae P. Biotechnol. Lett. 32, 701–705. http://dx.doi.org/10.1007/s10529–010–0210–3.